

ESI

Synthesis, crystallographic study and solid-state properties of metal-free perovskites with P-atom containing A-site cations

Yumi Matsuda,^a Rentaro Asai,^a Jumpei Moriguchi,^a Tomoyuki Akutagawa,^b Atsuko Masuya-Suzuki^a and Ryo Tsunashima*^a

1. Experimental procedures

2. XRD

3. TG-DTA

4. DSC

5. Dielectric properties of p-Br

6. Crystallographic consideration

1. Experimental Procedures

1-1 Materials

p-Br

Crystallisation was performed by mixing pta (10 mmol) with HBr (20 mmol) in an aqueous solution (3 mL) and evaporating it in air for 3-7 days to obtain high-quality, colourless block crystals (yields; 16.0 %).

Elemental Anal (%): calc C 17.29, H 4.35, N 13.44 for $(C_6H_{14}N_3P)(NH_4)Br_3$; found: C 17.418, H 4.469, N 13.477

FT-IR: ν_{max}/cm^{-1} 3118s, 2945s, 1375vs, 989s, 798s and 569s (Figure S1-1).

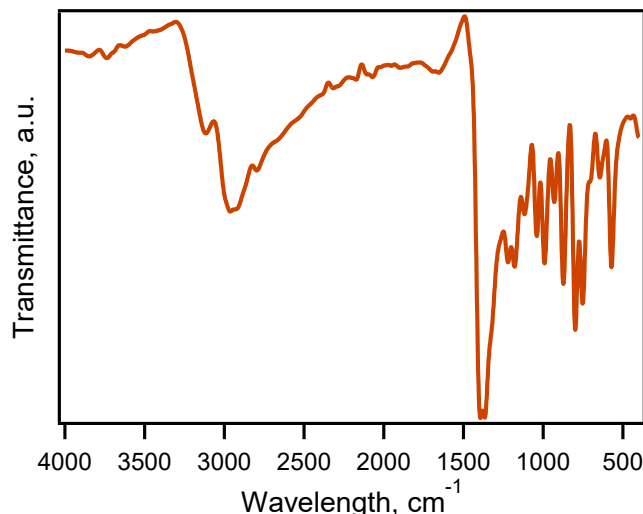


Figure S1-1. IR spectrum of p-Br.

p-I

Crystallisation was performed by mixing pta (10 mmol) with HI (20 mmol) in an aqueous solution (5 mL) and evaporating it in air for 3-7 days to obtain high-quality, colourless block crystals (yields; 23.9 %).

Elemental Anal (%): calc C 12.92, H 3.25, N 10.04 for $(C_6H_{14}N_3P)(NH_4)I_3$; found: C 13.31, H 3.042, N 10.03

FT-IR: ν_{max}/cm^{-1} 3116s, 2976s, 1367vs, 982s, 789s and 559s (Figure S1-2).

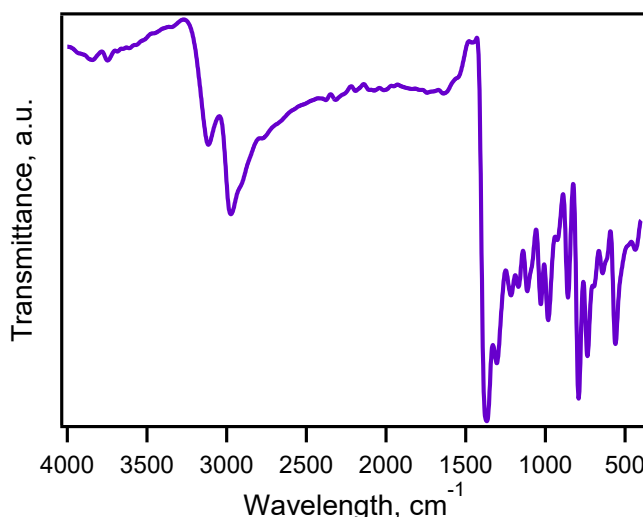


Figure S1-2. IR spectrum of p-I.

p-BF₄

Crystallisation was performed by mixing pta (10 mmol) with HBF₄ (20 mmol) in an aqueous solution (10 mL) and evaporating it in air for 3-7 days to obtain high-quality, colourless block crystals (yields; 38.8 %).

Elemental Anal (%): calc C 16.47, H 4.15, N 12.80 for (C₆H₁₄N₃P)(NH₄)(BF₄)₃; found: C 16.947, H 4.244, N 12.908

FT-IR: $\nu_{\text{max}}/\text{cm}^{-1}$ 3311s, 3169s, 1427s, 1003vs, 795s and 525s (Figure S1-3).

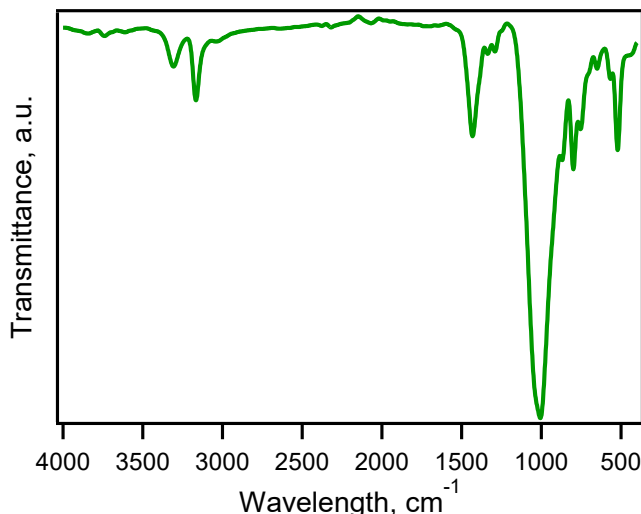


Figure S1-3. IR spectrum of p-BF₄.

1-2 Crystallography

A suitable crystal was selected and putted on a XtaLAB Synergy R, DW system, HyPix diffractometer. The crystal was kept during data collection. Using Olex2 [1], the structure was solved with the SHELXT [2] structure solution program using Intrinsic Phasing and refined with the SHELXL [3] refinement package using Least Squares minimisation.

1. Dolomanov, O.V., Bourhis, L.J., Gildea, R.J., Howard, J.A.K. & Puschmann, H. (2009), *J. Appl. Cryst.* 42, 339-341.
2. Sheldrick, G.M. (2015). *Acta Cryst. A*71, 3-8.
3. Sheldrick, G.M. (2015). *Acta Cryst. C*71, 3-8.

1-3 Measurements

PXRD. PXRD at room temperature was performed using a Rigaku Mini Flex 600.

DSC. Rigaku Thermo plus REVO2 Differential Scanning Calorimeter Measurements were conducted in an N₂ atmosphere at a sweep rate of 10 K min⁻¹.

Complex permittivity. Measurements were made in the frequency range of 100–1 MHz using an E4980AL Precision LCR Meter (KEYSIGHT). The measurements were performed with handmade cryostat under vacuum, and the temperature was controlled using a LakeShore 335 Temperature Controller.

P-E Hysteresis. Measurements were performed using a RADIANT Precision LC II instrument.

2. XRD

Crystallographic data characterized by SC-XRD were summarized in Table S2-1 and S2-2. Figure S2-1 to S2-4 are pictures of crystal structure of **p-Br**, **p-I**, and **p-BF₄**. Figure S2-5, S2-6, and S2-7 are PXRD patterns of **p-Br**, **p-I**, and **p-BF₄**.

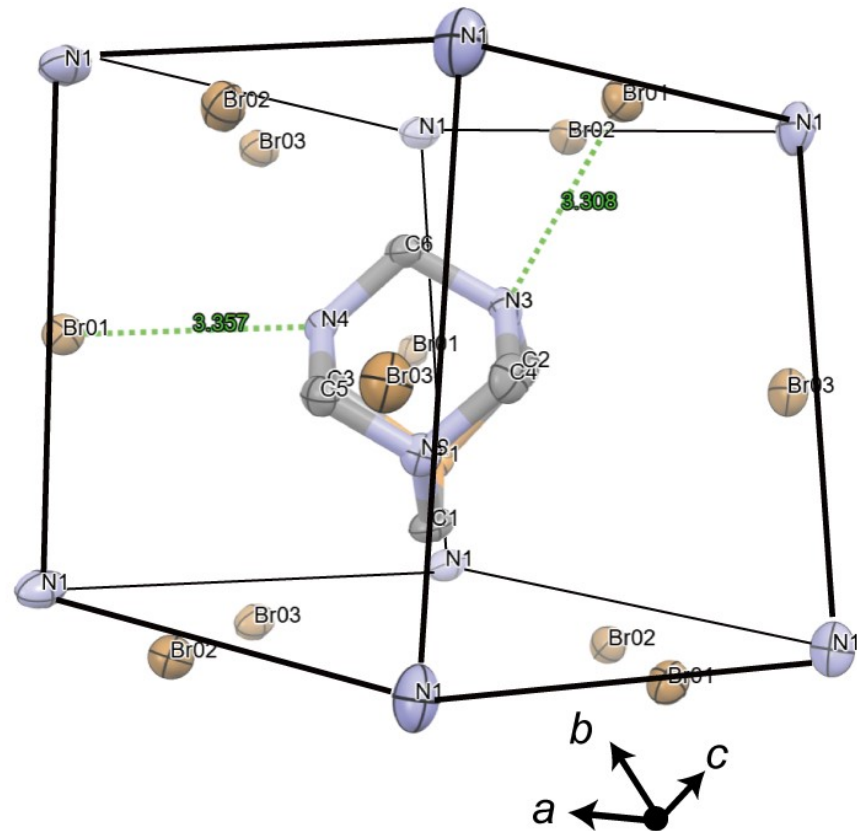


Figure S2-1. Structure of **p-Br** (253 K) picked for ABX₃ structural frame.

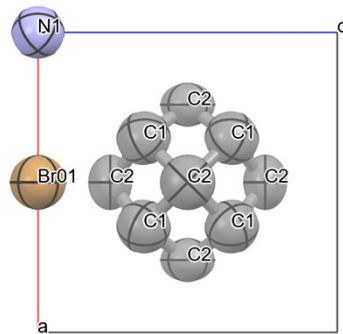


Figure S2-2. Structure of **p-Br** (415 K) in the unit cell.

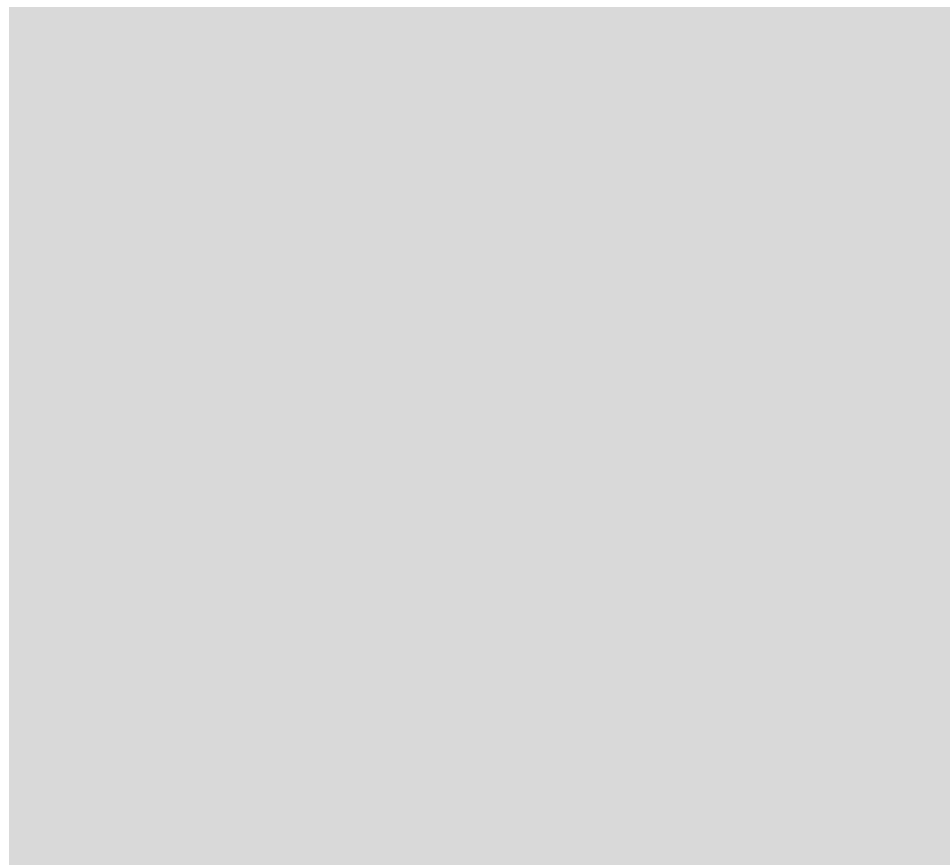


Figure S2-3. Structure of **p-I** (253 K) picked for ABX_3 structural frame.

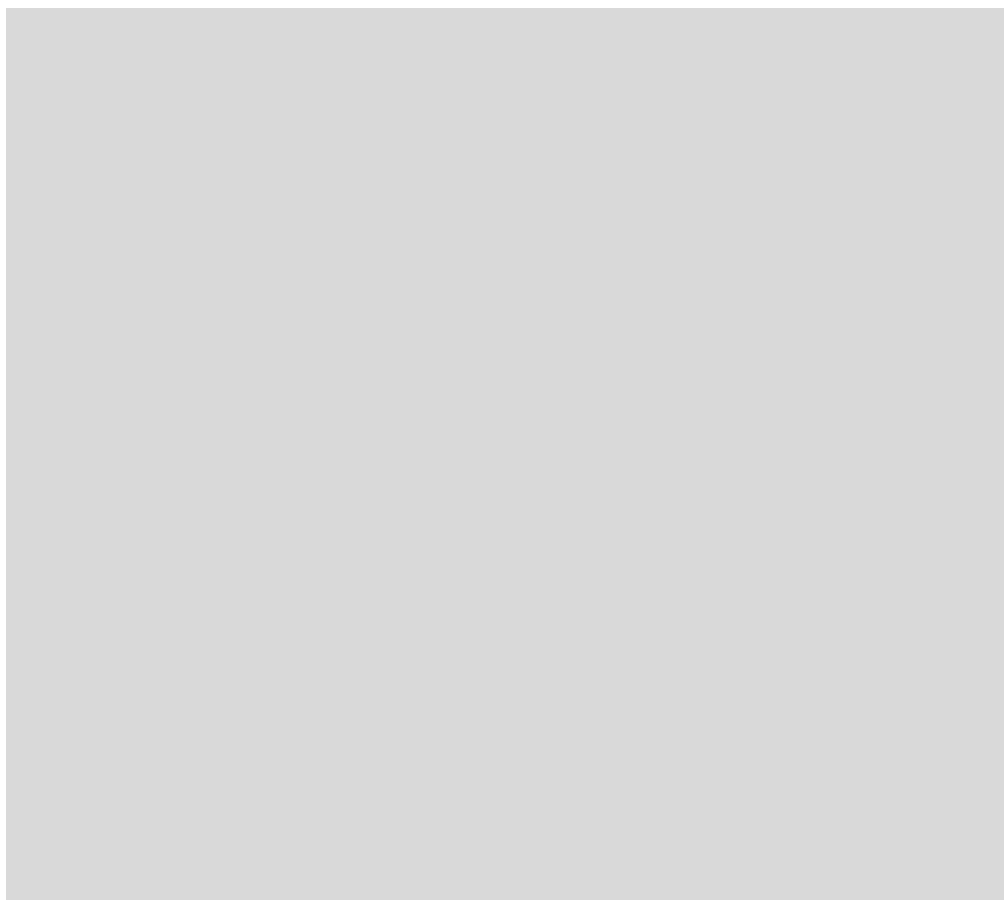


Figure S2-4. Structure of **p**-BF₄ (233 K) picked for ABX₃ structural frame.

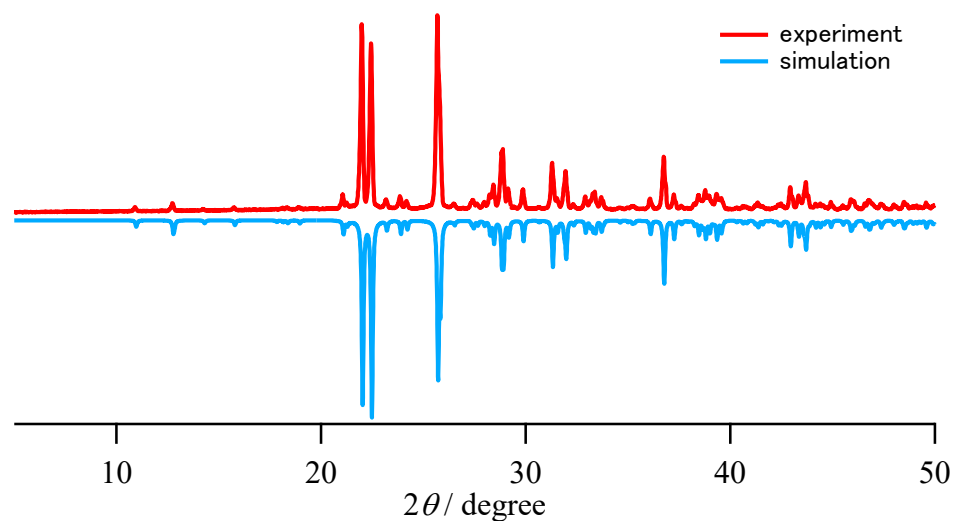


Figure S2-5. powder XRD pattern of **p**-Br.

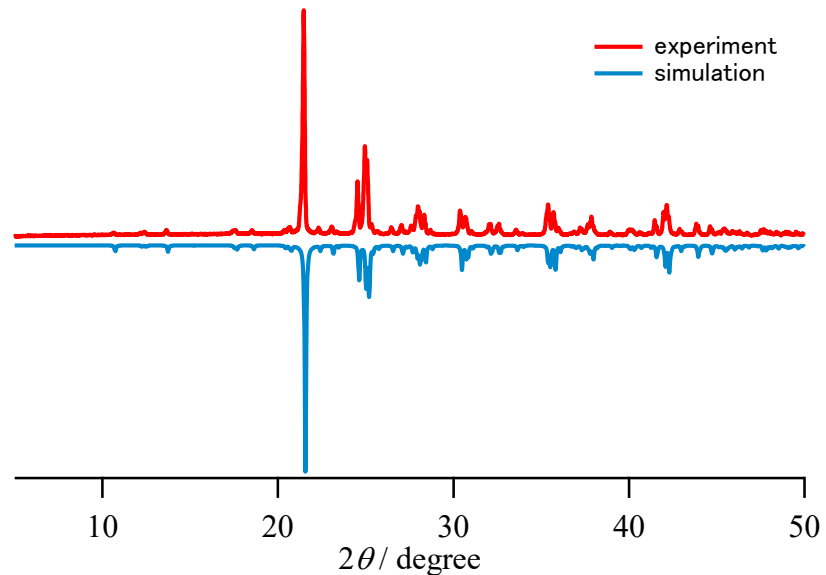


Figure S2-6. powder XRD pattern of p-I

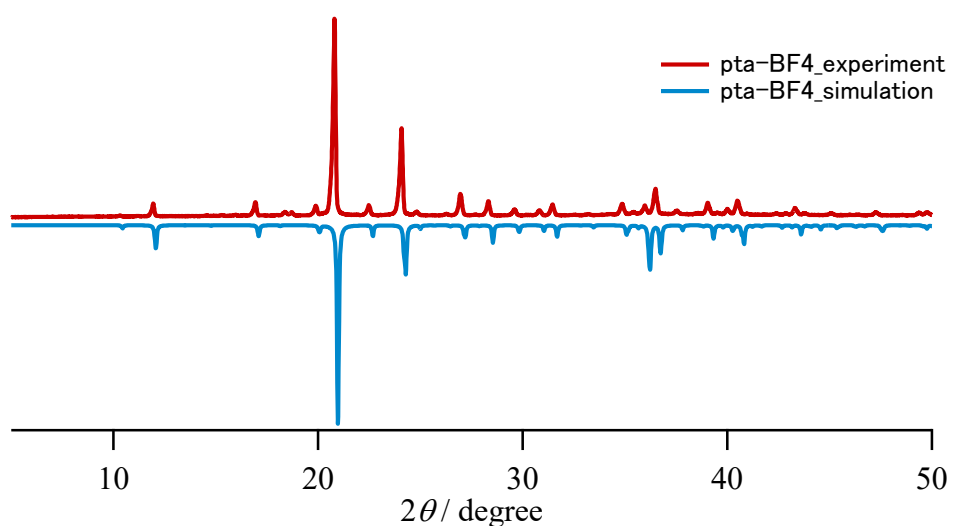


Figure S2-7. powder XRD pattern of p-BF₄.

2-2 Temperature variable SC-XRD of p-Br: SC-XRD analysis were performed with raising temperature over order-disorder phase transition. Structures were solved with orthorhombic $Pna2_1$ ($< 391\text{K}$) and cubic $Pm-3m$ ($\geq 391 \text{ K}$). Crystal structure at 391 K was not solved by orthorhombic. R_{int} value is 0.1375 for orthorhombic system, higher than 0.0439 for cubic system (Figure S2-8). Crystallographic data summarised in Table S2-1.

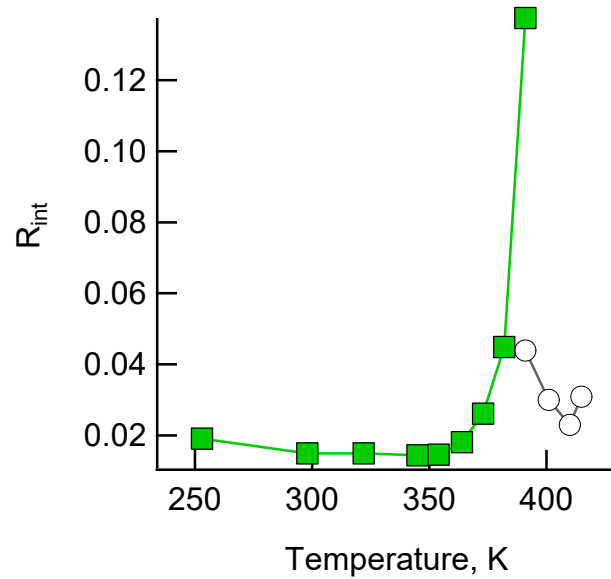


Figure S2-8. Temperature dependence of R_{int} of p-Br.

Table S2-1. Crystallographic data of p-Br

Compounds	p-Br													
Empirical formula	$C_6H_{18}Br_3N_4P$										$Br_3C_{12.6}N$	$Br_3C_{12.6}N$	$Br_3C_{12.3}N$	$Br_3C_{14}N$
Formula weight	416.94										405.07	403.38	401.46	421.88
Temperature/K	253	298	322	345	354	364	373	382	391	401	410	415		
Crystal system	orthorhombic										cubic			
Space group	$Pna\bar{2}_1$										$Pm\cdot3m$			
$a/\text{\AA}$	13.7604(3)	13.7833(4)	13.7974(4)	13.8098(4)	13.8180(5)	13.8355(5)	13.8318(6)	13.8322(8)	6.9497(9)	6.9822(4)	7.0028(4)	7.0146(4)		
$b/\text{\AA}$	9.9259(3)	9.9419(3)	9.9483(3)	9.9529(3)	9.9528(4)	9.9594(4)	9.9497(4)	9.9354(7)	-	-	-	-		
$c/\text{\AA}$	9.6119(3)	9.6453(3)	9.6610(3)	9.6797(4)	9.6881(4)	9.7006(4)	9.7003(6)	9.7055(8)	-	-	-	-		
$\alpha/^\circ$	-	-	-	-	-	-	-	-	-	-	-	-		
$\beta/^\circ$	-	-	-	-	-	-	-	-	-	-	-	-		
$\gamma/^\circ$	-	-	-	-	-	-	-	-	-	-	-	-		
Volume/ \AA^3	1312.84(6)	1321.72(7)	1326.08(7)	1330.45(8)	1332.38(9)	1336.68(9)	1334.98(11)	1333.81(16)	335.66(13)	340.39(6)	343.41(6)	345.15(6)		
Z	4	4	4	4	4	4	4	4	1	1	1	1		
$\rho_{\text{calc}} \text{ g/cm}^3$	2.109	2.095	2.088	2.082	2.079	2.072	2.074	2.076	2.004	1.968	1.941	2.03		
μ/mm^{-1}	9.314	9.251	9.221	9.19	9.177	9.148	9.159	9.167	8.987	8.861	8.783	8.744		
F(000)	808	808	808	808	808	808	808	808	188	187	186	196		
Crystal size/mm ³	0.24 × 0.2 × 0.16	0.19 × 0.18 × 0.16	0.22 × 0.18 × 0.16	0.19 × 0.19 × 0.14	0.2 × 0.19 × 0.15	0.22 × 0.19 × 0.16	0.25 × 0.22 × 0.17	0.25 × 0.22 × 0.17	0.22 × 0.21 × 0.15	0.22 × 0.21 × 0.16	0.24 × 0.2 × 0.16	0.27 × 0.19 × 0.16		
Radiation	Mo K α ($\lambda = 0.71073$)													
2 Θ range for data collection/°	5.9 to 60.46	5.884 to 52.73	5.878 to 52.732	5.87 to 52.734	5.868 to 52.744	5.862 to 61.152	5.866 to 61.17	5.868 to 61.168	5.862 to 60.822	5.834 to 61.188	5.818 to 52.514	5.808 to 61.212		
Index ranges	-19 ≤ h ≤ 15, -13 ≤ k ≤ 10, -12 ≤ l ≤ 8	-15 ≤ h ≤ 17, -10 ≤ k ≤ 12, -12 ≤ l ≤ 8	-15 ≤ h ≤ 17, -1 ≤ k ≤ 12, -12 ≤ l ≤ 8	-15 ≤ h ≤ 17, -10 ≤ k ≤ 12, -12 ≤ l ≤ 8	-15 ≤ h ≤ 17, -10 ≤ k ≤ 12, -12 ≤ l ≤ 8	-15 ≤ h ≤ 19, -10 ≤ k ≤ 13, -12 ≤ l ≤ 8	-19 ≤ h ≤ 15, -13 ≤ k ≤ 10, -12 ≤ l ≤ 8	-19 ≤ h ≤ 15, -13 ≤ k ≤ 10, -12 ≤ l ≤ 8	-2 ≤ h ≤ 8, -8 ≤ k ≤ 8, -7 ≤ l ≤ 9	-2 ≤ h ≤ 8, -8 ≤ k ≤ 8, -7 ≤ l ≤ 9	-2 ≤ h ≤ 7, -8 ≤ k ≤ 8, -7 ≤ l ≤ 8	-8 ≤ h ≤ 8, -9 ≤ k ≤ 7, -8 ≤ l ≤ 2		
Reflections collected	5489	5100	5109	5122	5119	5578	5607	5572	1499	1523	1404	1544		
Independent reflections	2279 [R _{int} = 0.0191, R _{sigma} = 0.0233]	2061 [R _{int} = 0.0149, R _{sigma} = 0.0183]	2060 [R _{int} = 0.0149, R _{sigma} = 0.0193]	2067 [R _{int} = 0.0144, R _{sigma} = 0.0187]	2067 [R _{int} = 0.0146, R _{sigma} = 0.0190]	2370 [R _{int} = 0.0181, R _{sigma} = 0.0216]	2361 [R _{int} = 0.0261, R _{sigma} = 0.0251]	2368 [R _{int} = 0.0449, R _{sigma} = 0.0359]	132 [R _{int} = 0.0439, R _{sigma} = 0.0654]	134 [R _{int} = 0.0439, R _{sigma} = 0.0654]	101 [R _{int} = 0.0300, R _{sigma} = 0.0162]	135 [R _{int} = 0.0230, R _{sigma} = 0.0195]	101 [R _{int} = 0.0230, R _{sigma} = 0.0160]	135 [R _{int} = 0.0201]
Data/restraints/parameters	2279/1/140	2061/1/140	2060/11/139	2067/11/139	2067/11/139	2370/11/139	2361/11/148	2368/11/158	132/0/13	134/0/12	101/0/12	135/0/10		
Goodness-of-fit on F ²	1.117	1.069	1.051	1.053	1.047	1.069	1.153	1.023	1.083	1.07	1.434	1.101		
Final R indexes [$I >= 2\sigma(I)$]	$R_1 = 0.0224, wR_2 = 0.0509$	$R_1 = 0.0481, wR_2 = 0.1258$	$R_1 = 0.0491, wR_2 = 0.1299$	$R_1 = 0.0503, wR_2 = 0.1344$	$R_1 = 0.0499, wR_2 = 0.1349$	$R_1 = 0.0451, wR_2 = 0.1106$	$R_1 = 0.0582, wR_2 = 0.1283$	$R_1 = 0.0870, wR_2 = 0.1889$	$R_1 = 0.0488, wR_2 = 0.1193$	$R_1 = 0.0404, wR_2 = 0.1199$	$R_1 = 0.0620, wR_2 = 0.1271$	$R_1 = 0.0729, wR_2 = 0.2556$		
Final R indexes [all data]	$R_1 = 0.0237, wR_2 = 0.0512$	$R_1 = 0.0492, wR_2 = 0.1268$	$R_1 = 0.0505, wR_2 = 0.1310$	$R_1 = 0.0522, wR_2 = 0.1363$	$R_1 = 0.0525, wR_2 = 0.1367$	$R_1 = 0.0513, wR_2 = 0.1137$	$R_1 = 0.0681, wR_2 = 0.1331$	$R_1 = 0.1106, wR_2 = 0.2076$	$R_1 = 0.0760, wR_2 = 0.1301$	$R_1 = 0.0657, wR_2 = 0.1422$	$R_1 = 0.0717, wR_2 = 0.1317$	$R_1 = 0.1203, wR_2 = 0.2999$		
Largest diff. peak/hole / e Å ⁻³	0.46/-0.74	0.76/-1.11	0.60/-1.00	0.69/-0.88	0.76/-0.80	1.04/-0.63	1.63/-0.81	2.60/-1.13	0.32/-0.62	0.16/-0.22	0.30/-0.19	0.74/-0.43		
Flack parameter	0.025(8)	0.018(13)	0.007(14)	0.012(12)	0.013(11)	0.005(8)	0.071(15)	0.10(3)	-	-	-	-		

Table S2-2. Crystallographic data of p-I and p-BF₄.

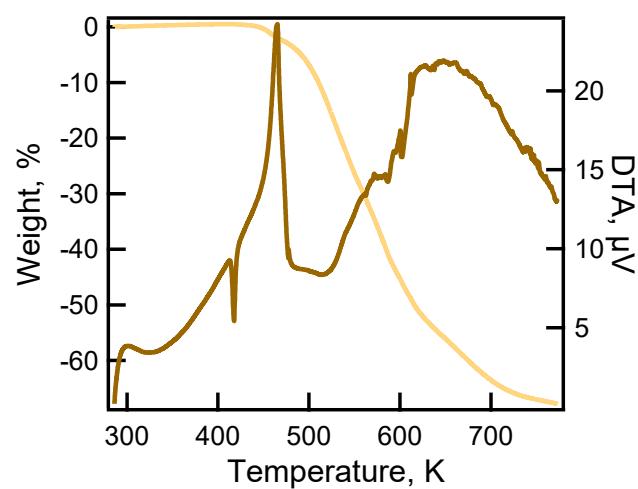
Compounds	p-I			p-BF ₄	
Empirical formula	C ₆ H ₁₈ I ₃ N ₄ P			C ₆ H _{17.72} B ₃ F ₁₂ N ₄ P	
Formula weight	557.91			437.36	
Temperature/K	253	298	410	233	391
Crystal system	orthorhombic			tetragonal	
Space group	Cmce			P 4 ₂ /n	
a/Å	14.1395(5)	14.1583(4)	14.2452(5)	10.35730(10)	10.4847(3)
b/Å	14.4681(5)	14.4657(4)	14.5204(6)	10.35730(10)	10.4847(3)
c/Å	14.2255(4)	14.2413(3)	14.3176(5)	14.6992(3)	14.8469(7)
α/°	-	-	-	-	-
β/°	-	-	-	-	-
γ/°	-	-	-	-	-
Volume/Å ³	2910.13(17)	2916.76(13)	2961.54(19)	1576.84(4)	1632.10(11)
Z	8	8	8	4	4
ρ _{calc} g/cm ³	2.547	2.541	2.48	1.842	1.78
μ/mm ⁻¹	6.531	6.516	6.417	0.306	s
F(000)	2048	2048	2022	879	875
Crystal size/mm ³	0.31 × 0.24 × 0.17	0.29 × 0.25 × 0.17	0.32 × 0.26 × 0.15	0.23 × 0.22 × 0.11	0.233 × 0.216 × 0.11
Radiation	Mo Kα (λ = 0.71073)			Mo Kα (λ = 0.71073)	
2Θ range for data collection/°	4.942 to 52.738	4.938 to 52.742	4.914 to 52.74	3.932 to 60.486	4.756 to 60.366
Index ranges	-17 ≤ h ≤ 14, -17 ≤ k ≤ 18, -14 ≤ l ≤ 17	-17 ≤ h ≤ 17, -18 ≤ k ≤ 15, -17 ≤ l ≤ 17	-17 ≤ h ≤ 17, -16 ≤ k ≤ 18, -17 ≤ l ≤ 17	-14 ≤ h ≤ 13, -14 ≤ k ≤ 14, -19 ≤ l ≤ 20	-9 ≤ h ≤ 13, -13 ≤ k ≤ 12, -17 ≤ l ≤ 20
Reflections collected	6432	6393	6301	28348	7333
Independent reflections	1547 [R _{int} = 0.0244, R _{sigma} = 0.0198]	1542 [R _{int} = 0.0197, R _{sigma} = 0.0146]	1564 [R _{int} = 0.0387, R _{sigma} = 0.0224]	2130 [R _{int} = 0.0451, R _{sigma} = 0.0184]	2002 [R _{int} = 0.0121, R _{sigma} = 0.0141]
Data/restraints/parameters	1547/9/111	1542/9/115	1564/15/116	2130/10/143	2002/10/198
Goodness-of-fit on F ²	1.092	1.136	1.089	1.069	1.093
Final R indexes [I>=2σ (I)]	R ₁ = 0.0211, wR ₂ = 0.0522	R ₁ = 0.0170, wR ₂ = 0.0436	R ₁ = 0.0339, wR ₂ = 0.0937	R ₁ = 0.0589, wR ₂ = 0.1591	R ₁ = 0.0638, wR ₂ = 0.1990
Final R indexes [all data]	R ₁ = 0.0224, wR ₂ = 0.0527	R ₁ = 0.0177, wR ₂ = 0.0439	R ₁ = 0.0356, wR ₂ = 0.0953	R ₁ = 0.0623, wR ₂ = 0.1632	R ₁ = 0.0796, wR ₂ = 0.2220
Largest diff. peak/hole / e Å ⁻³	0.93/-0.55	0.61/-0.55	0.83/-0.89	0.89/-0.33	0.34/-0.23
Flack parameter	-	-	-	-	-

Table S2-3. List of CCDC numbers

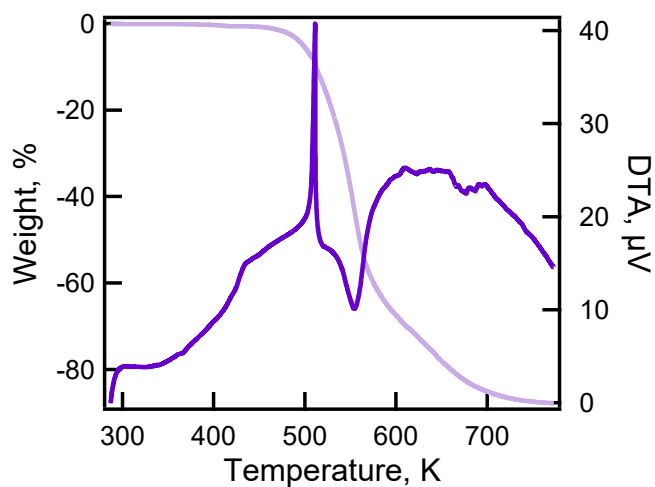
Sample	Temperature, K	Data name	CCDC number
p-Br	253	data_rt1225_inv	2424529
	298	data_pta-br_298k	2424525
	322	data_pta-br_322k	2424522
	345	data_pta-br_345k	2424521
	354	data_p-br_354k	2424524
	364	data_364k_rt	2424527
	373	data_373k_rt2_inv	2424523
	382	data_382k_rt1_inv	2424526
	391	data_391k_cubic_rt1	2424528
	401	data_401k_cubic_rt	2424519
p-I	410	data_m_pta-br_420_1	2424520
	415	data_pta-br_425_1	2424518
	253	p-i_253k	2424323
p-BF₄	298	data_p-i_298k	2424321
	410	data_p-i_410k	2424322
	233	data_p-bf4_233k	2424326
	391	data_p-bf4_391k	2424324

3 TG-DTA

(a)



(b)



(c)

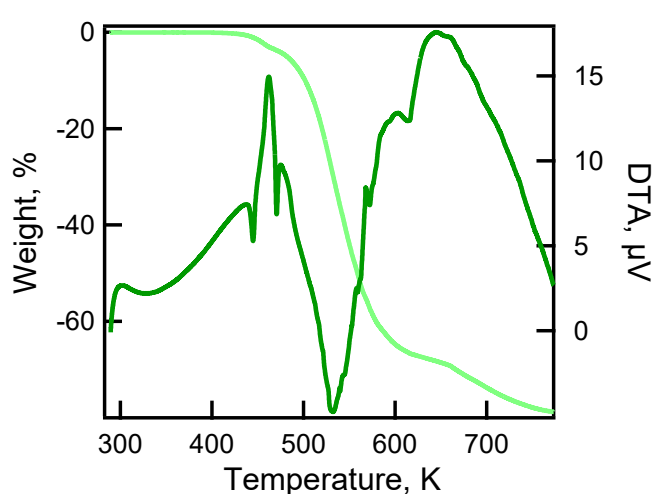
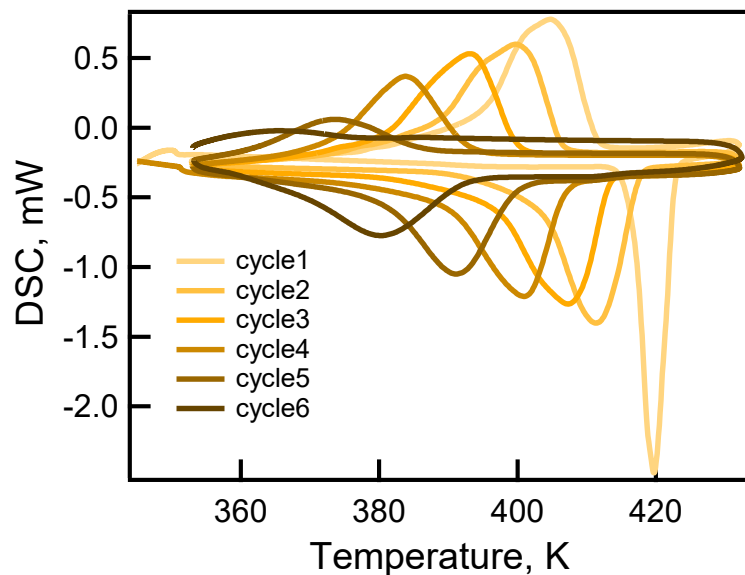


Figure S3-1. TG-DTA of (a) **p-Br**, (b) **p-I**, and (c) **p-BF₄**

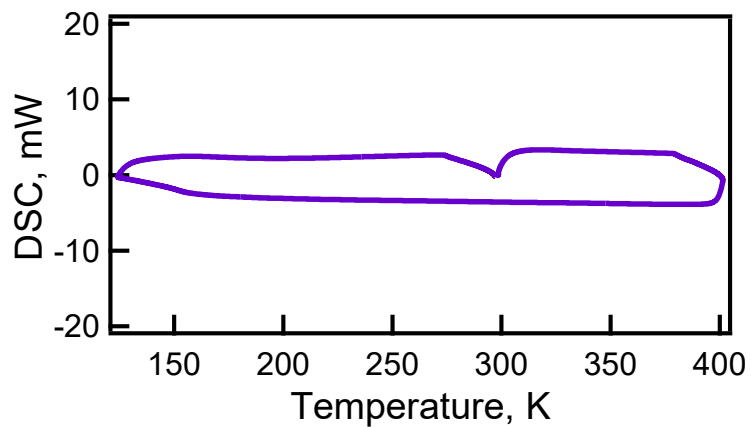
4. DSC

p-Br: For the initial heating process, ΔH , T_c , and entropy ΔS were 4.46 kJ mol^{-1} , 417 K , and $10.6 \text{ J mol}^{-1} \text{ K}^{-1}$, respectively

(a)



(b)



(c)

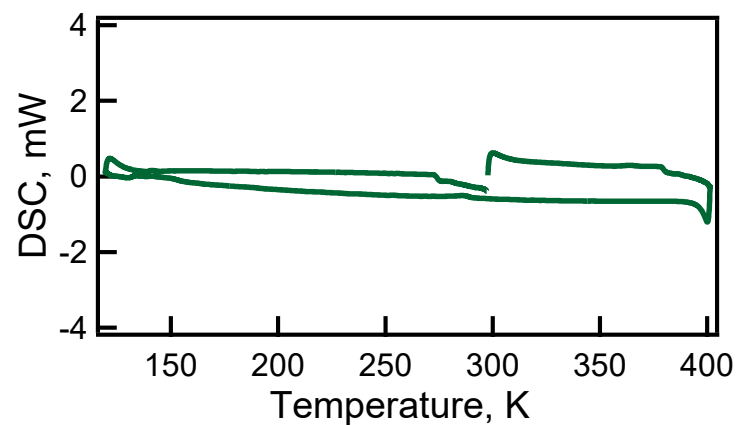


Figure S4-1. DSC of (a) p-Br, (b) p-I, and (c) p-BF₄

5. Dielectric properties of p-Br

5.1 Dielectric constant

Complex permittivity was characterized by impedance method using powder pellets of **p-Br**.

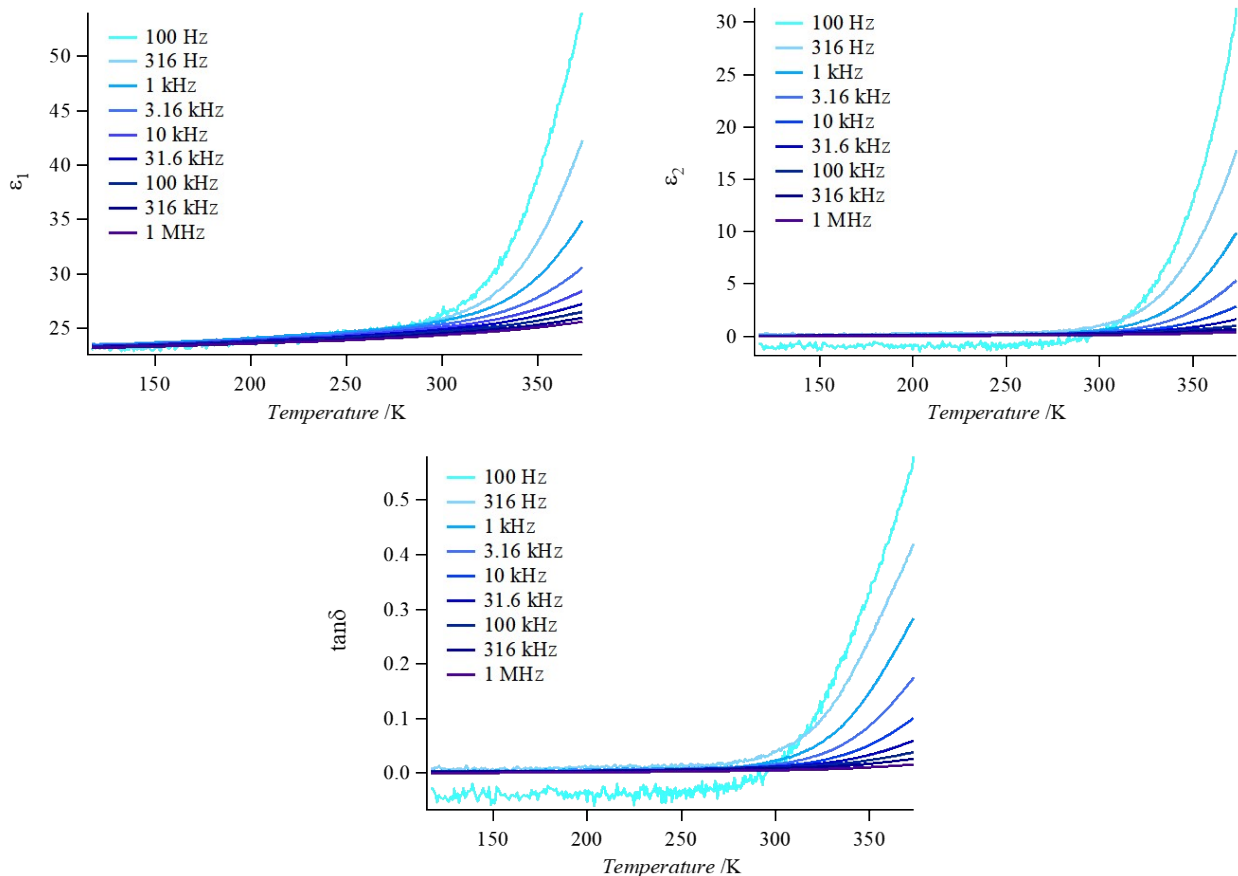


Figure S5-1. Temperature dependence (120-370 K) of real (ϵ_1) and imaginary (ϵ_2) parts of complex permittivity and tangent delta of **p-Br**.

5.2 Ferroelectric characterization of p-Br

The **p-Br** undergoes order-disorder transition from polar structure. This is typical behaviour for ferroelectric materials. However, obvious electric field switching of spontaneous polarization was not observed below 20.0 kV cm^{-1} at 1-100 Hz (Figure S5-2). We consider large leak current is possible of the single crystal and decomposition by heating samples.

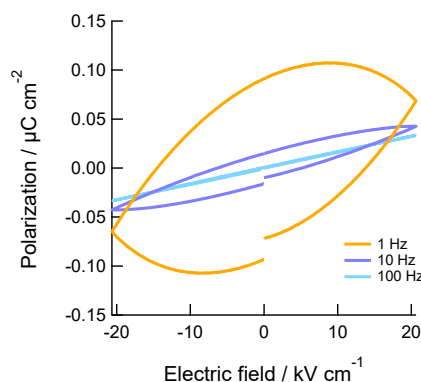


Figure S5-2. PE hysteresis at room temperature measured at 1, 10 and 100 Hz for a single crystal of **p-Br** along polar axis.

6. Crystallographic consideration

6.1 New tolerance factor

According to eq. 3, τ values were estimated and summarized in table S6-1.

Table S6-1. Summary of τ with $n_A = +2$ estimated for different A-site cations and X anion.

A-site cations	F	Cl	Br	I	BF ₄
hmta	3.38	3.72	3.83	3.99	4.07
pta	3.02	3.36	3.46	3.63	3.71
μ^+	0.90	1.24	1.34	1.51	1.59

6.2 Distortion index

Distortion index (D) was estimated by bond lengths defined by

$$D = \frac{1}{n} \sum_{i=1}^n \frac{|l_i - l_{av}|}{l_{av}}$$

where l_i is the distance from the central atom to the coordinating atom, and l_{av} is the average bond length.

6.3 Bond angle variance

Bond angle variance (A) was calculated by

$$\sigma^2 = \frac{1}{m-1} \sum_{i=1}^m (\phi_i - \phi_0)^2$$

where m and ϕ_0 are 12 and 90°, respectively.